Hyperactivity of mTORC1 or mTORC2-dependent signaling causes epilepsy downstream of somatic PTEN loss.

Erin R. Cullen[1*], Isabelle Mittelstadt[1], and Matthew C. Weston[1,2,3**.]

[1]Department of Neurological Sciences, Larner College of Medicine, University of Vermont, Burlington VT, 05405, USA.

[2]Fralin Biomedical Research Institute at VTC, Center for Neurobiology Research, Roanoke VA, 24016, USA

[3]School of Neuroscience, Virginia Polytechnic and State University, Blacksburg VA, 24060, USA

* Present address:

Columbia University Irving Medical Center
Hammer Health Sciences Building Room 601
701 W. 168th St
New York, NY 10032

** to whom correspondence should be addressed: mcweston7c@vt.edu

Abstract: Gene variants that hyperactivate PI3K-mTOR signaling in the brain lead to epilepsy and cortical malformations in humans. Some gene variants associated with these pathologies only hyperactivate mTORC1, but others, such as *PTEN*, *PIC3CA*, and *AKT*, hyperactivate both mTORC1- and mTORC2-dependent signaling. Previous work has established a key role for mTORC1 hyperactivity in mTORopathies, however, whether mTORC2 hyperactivity contributes is not clear. To test this, we inactivated mTORC1 and/or mTORC2 downstream of early *Pten* deletion in a new model of somatic Pten LOF in the cortex. Spontaneous seizures and epileptiform activity persisted despite mTORC1 or mTORC2 inactivation alone, but inactivating both mTORC1 and mTORC2 normalized pathology. These results suggest that hyperactivity of both mTORC1 and mTORC2 are sufficient to cause epilepsy, and that targeted therapies should aim to reduce activity of both complexes.

Introduction:

Genetic disruptions that hyperactivate mTOR activity, termed 'mTORopathies', cause macrocephaly, intractable childhood epilepsies, and behavioral presentations including autism spectrum disorders [1-4]. The mTOR kinase can function in two complexes, mTORC1 and mTORC2, each with unique downstream targets and upstream activators [5]. A unifying feature of mTORopathies is hyperactivation of mTORC1, which has led to the hypothesis that this complex and its effectors mediate disease phenotypes [6]. A subset of mTORopathies however, *(*e.g. those caused by variants in *PTEN*, *PIC3CA*, and *AKT)*, hyperactivate both mTORC1 and mTORC2 [7,8], and mTORC2 hyperactivity has also been reported in human TLE [9]. It is unclear whether mTORC2 hyperactivity contributes to, or can cause, disease phenotypes such as epilepsy.

PTEN LOF in neurons induces soma hypertrophy, increased dendritic branching, and synaptic hyperconnectivity [10,11]. These phenotypes resemble those observed in models of mTORC1-specific hyperactivation [12], and can be prevented with either the mTORC1 inhibitor rapamycin or loss of the mTORC1-specific protein Raptor [13]. Rapamycin also rescues epilepsy and mortality associated with *Pten* loss, even after epilepsy has been established, suggesting that mTORC1 hyperactivity underlies these phenotypes [14-16]. Thus, there is strong evidence that hyperactivation of mTORC1 downstream of PTEN disruption causes the macrocephaly, epilepsy, early mortality, and synaptic dysregulation observed in humans and model organisms [17].

There is also evidence against the mTORC1-centric hypothesis. Rapamycin may affect mTORC2 activity at high doses or over long periods of time [18,17], and mTORC2 regulates synapse function, neuronal size, and cytoskeletal organization independent of mTORC1 [19,20]. In a mouse model in which *Pten* was inactivated in forebrain neurons in early adulthood, mTORC2 inhibition, but not mTORC1 inhibition, rescued seizures and behavioral abnormalities. In this model, epilepsy was dissociated from macrocephaly, which was rescued by mTORC1 inhibition but not mTORC2 inhibition [21]. However, mTORC2 inactivation did not normalize spontaneous seizures or seizure susceptibility in a model of *Pten* loss in dentate granule neurons [22]. Thus, there is conflicting evidence about whether mTORC1 or mTORC2 hyperactivity causes epilepsy downstream of *Pten* loss.

To address this, we suppressed mTORC1 and mTORC2 activity alongside PTEN LOF by inducing simultaneous deletion of *Raptor* or *Rictor*, whose protein products are unique and essential components of mTORC1 and mTORC2, respectively, in a model of somatic PTEN LOF in the cortex. In this model, epilepsy could be rescued by concurrent mTORC1 and mTORC2 inactivation, but persisted when either gene remained intact, suggesting that hyperactivity of either complex can lead to neuronal hyperexcitability and epilepsy.

Results:

Generation of a developmental brain somatic mosaic model of PTEN LOF. To model the epileptogenic somatic mutations often observed in mTORopathies [23,24], we injected an AAV9 virus expressing GFP and Cre under control of the *hSyn* promoter into one hemisphere of the cortex of *Pten*$^{(fl/fl)}$, *Pten*$^{(fl/fl)}$-*Raptor*$^{(fl/fl)}$, *Pten*$^{(fl/fl)}$-*Rictor*$^{(fl/fl)}$, and *Pten*$^{(fl/fl)}$-*Raptor*$^{(fl/fl)}$-*Rictor*$^{(fl/fl)}$ mice at P0 (Fig. 1A). Green fluorescent protein (GFP) was expressed in neurons throughout the cortical layers in all experimental animals, but largely confined to one cortical hemisphere and the underlying hippocampus (Fig. 1B). The percentage of cells that were GFP+ was similar across groups, although there was a decrease in cell density in the Pten LOF and Pten-Rictor LOF groups [25] (Fig. 1C).

We analyzed the impact of Pten, Raptor, and Rictor LOF on mTORC1 and mTORC2 activity in the affected hemisphere using quantitative immunohistochemistry. Phospho-S6 levels, which report mTORC1 activity through S6K1, were increased from Controls in Pten LOF and Pten-Rictor LOF brains, but rescued in Pten-Raptor LOF brains (Fig. 1D$_1$). Phospho-Akt (S473) levels, which report mTORC2 activity, were increased in Pten LOF and Pten-Raptor LOF but normalized in Pten-Rictor LOF brains (Fig. 1D$_2$). Levels of both pS6 and pAkt were not different from Controls in Pten-Raptor-Rictor LOF brains. These results indicate that Pten LOF hyperactivates both mTORC1 and mTORC2 in this model, and that these increases in activity are independently rescued by mTORC1 and mTORC2 inactivation.

Raptor and/or Rictor LOF attenuate Pten LOF-induced macrocephaly. Macrocephaly and neuronal hypertrophy are well-characterized sequelae of deficient PTEN signaling in patients and mouse models [26,27]. In mouse models of Pten LOF, these phenotypes can be rescued by rapamycin treatment or Raptor LOF [21,28,17,13]. Here, cortical thickness was increased in Pten LOF and rescued to Control levels by Raptor LOF, Rictor LOF, or combined Raptor-Rictor LOF (Fig. 2A-B). In individual neurons Pten LOF caused a ≈100% increase in mean soma size versus Control. Pten-Rictor LOF significantly reduced soma size from Pten LOF levels, but still showed a 60% increase over Controls. Soma size in Pten-Raptor LOF and Pten-Raptor-Rictor LOF neurons did not significantly differ from Controls (Fig. 2C).

Concurrent mTORC1/2 inactivation, but neither alone, rescues epilepsy and interictal EEG abnormalities in focal Pten LOF. Next, we measured epileptic brain activity with video-EEG to determine the ability of mTORC1 or mTORC2 activity to rescue this key feature of mTORopathies, Generalized seizures (GS) were observed in 0/9 Control, 4/7 Pten LOF, 2/6 Pten-Raptor LOF, 2/7 Pten-Rictor LOF, and 0/6 Pten-Raptor-Rictor LOF animals. GS events were longer-lasting in Pten-

Raptor LOF animals than in Pten LOF or Pten-Rictor LOF animals (Fig. 3A). GS did not appear to be correlated with mTOR pathway activity (Supplementary Figure 2).

The most striking and consistent type of epileptic brain activity in the Pten LOF animals was frequent 5-7 Hz spike trains lasting 3 seconds or more, which fit previous characterizations of spike-and-wave discharges (SWDs) in rodents [29]. SWDs were observed in all Pten LOF, Pten-Raptor LOF, and Pten-Rictor LOF animals, and in 3/9 Control and 3/6 Pten-Raptor-Rictor LOF animals. The frequency of SWDs in Pten LOF, Pten-Raptor LOF, and Pten-Rictor LOF animals was significantly higher than Controls, but Pten-Raptor-Rictor LOF completely blocked this increase. Pten-Rictor LOF animals had a lower frequency of SWD events than Pten LOF animals (Fig. 3B), indicating a partial rescue. Taken together, these data indicate inactivating mTORC1 provides no protection against *Pten* loss-induced epilepsy, and may even exacerbate it. mTORC2 inactivation provides some protection, but only concurrent mTORC1 and mTORC2 inactivation can prevent it.

In addition to epileptic activity, we also found that Pten LOF caused obvious alterations in features of the interictal EEG. To quantify these changes, we measured EEG coastline, absolute mean amplitude, and power spectra of the EEG. Coastline, mean amplitude, and total power were all significantly increased by Pten LOF, and these changes were not significantly reduced by Pten-Raptor or Pten-Rictor LOF. Pten-Raptor-Rictor LOF, however, reduced these increases to Control levels. Correspondingly, EEG power was increased in Pten LOF animals (Fig. 4A; Table 1A). This increase was normalized by Pten-Raptor-Rictor LOF, but not by Pten-Raptor LOF or Pten-Rictor LOF. Pten-Raptor-Rictor LOF did not fully rescue a rightward shift in normalized EEG band power (Fig. 4B; Table 1B).

Discussion:

Convergent discoveries have positioned mTORopathies as prime candidates for a precision medicine approach [30,31]. There has been some clinical success with rapamycin analogues [32], but preclinical animal studies have suggested ways to further improve the selectivity and efficacy of the targets [12]. For the subset of mTORopathies in which mTORC1 but not mTORC2 signaling is hyperactive, selective inhibition of mTORC1 and its downstream effectors rescues many animal phenotypes, including seizures [33,34]. Studies using rapamycin as an mTORC1 inhibitor also came to this conclusion in Pten LOF models, but potential inhibition of mTORC2 and the finding that genetic inhibition of mTORC1 via *Raptor* deletion did not stop seizures, whereas inhibition of mTORC2 did [21], challenged this view. Here, we tested whether mTORC1 or mTORC2 inhibition alone were sufficient to block disease phenotypes in a model of somatic Pten LOF. Neither was, which agrees with previous findings that seizures persist in both Pten-Raptor LOF and Pten-Rictor LOF animals in

separate model systems [21,22]. This data could be interpreted as suggesting that epilepsy downstream of Pten LOF can proceed via mTORC-independent mechanisms, such as elevated ß-catenin or its protein phosphatase activity [25,35]. However, we found that simultaneous mTORC1 and mTORC2 inhibition corrected all of the pathological features of our model except for a rightward shift in relative EEG power (Fig. 4B). This suggests that epilepsy can be caused by hyperactivity of either mTORC1 or mTORC2-dependent signaling downstream of Pten LOF, but not alternative pathways. Future studies should determine whether this is also true for other gene variants that hyperactivate both mTORC1 and mTORC2, as well in other models that have fully penetrant generalized seizures.

Epilepsy in Pten-Rictor LOF mice likely emerges via mechanisms similar to those in mTOR pathway variants such as TSC that hyperactivate mTORC1 but not mTORC2, although additional effects of mTORC2 inactivation may contribute [22]. Epilepsy in Pten-Raptor LOF occurs in the absence of macrocephaly, a hallmark of mTORC1 hyperactivity, possibly due to mTORC2 hyperactivity's effect on synaptic transmission [20]. Roles for both complexes in emergent neural network function are corroborated by findings that behavior can be altered by either mTORC1 or mTORC2 inactivation [36]. Rapamycin derivatives are somewhat selective for mTORC1 [37,38] and are currently being tested in the clinic to treat mTORopathies and PTEN-related disorders [18]. Even more selective targeting of mTORC1 than can be achieved through rapamycin and its derivatives has been proposed as a way to effectively treat disease with fewer side effects [39]. Our data suggest that this may only be true for mTORopathies that only hyperactive mTORC1. For others, including *PTEN*, *PIK3CA*, and *AKT*, dual inhibitors or inhibitors of PI3K, which are being tested preclinically [40-42], are likely to be required.

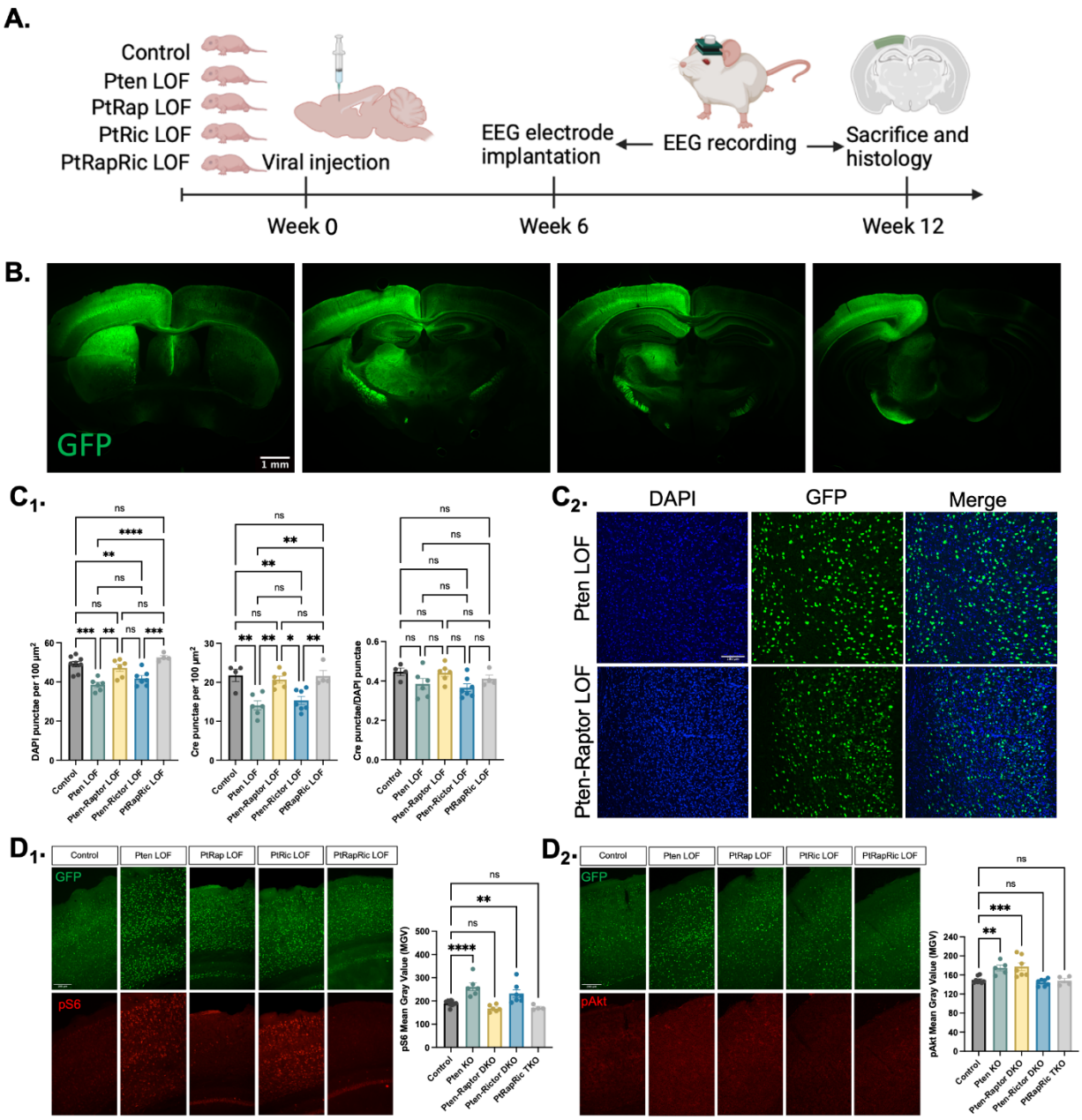

Figure 1. Characterization of the focal cortical Pten LOF model.

A) Experimental timeline showing induction of *hSyn*-Cre-GFP or Control *hSyn*-GFP AAV at P0 and EEG recording in adulthood. B) Representative images of GFP expression in a Control mouse brain, demonstrating expression predominantly in one hemisphere of the cortex. C_1) Quantification of lesion severity and neuron density in Cre-expressing animals. There were fewer Cre-expressing neurons per unit area in the *Pten* LOF and *Pten-Rictor* LOF groups, which was at least partially attributable to a decrease in cell density in these groups. No significant differences in Cre expression remained when Cre expression was calculated based on cell density rather than area. C_2) Representative images of DAPI and Cre fluorescence in the cortex of *Pten* LOF and *Pten-Raptor* LOF animals. Cell density and Cre density in *Pten-Raptor* LOF animals was indistinguishable from Controls. D_1) Phospho-S6, a marker of mTORC1 activity, was increased by *Pten* LOF and reduced to control levels by concurrent *Raptor* LOF. Phospho-S6 was also increased from Control levels in *Pten-Rictor* LOF, indicating that mTORC1 hyperactivity was not normalized by *Rictor* LOF. Combined *Raptor*/*Rictor* LOF also normalized phospho-S6 expression. D_2) phospho-Akt, a marker of mTORC2 activity, was increased in *Pten* LOF and normalized by *Rictor* LOF, but not by *Raptor* LOF. Combined *Raptor*/*Rictor* LOF also normalized phospho-Akt expression. Error bars show mean ± s.e.m. ns indicates $p>0.05$, * indicates $p<0.05$, ** indicates $p<0.01$, *** indicates $p<0.001$, and **** indicates $p<0.0001$ as assessed by one-way ANOVA with Tukey multiple comparisons correction. Diagram created with BioRender.com.

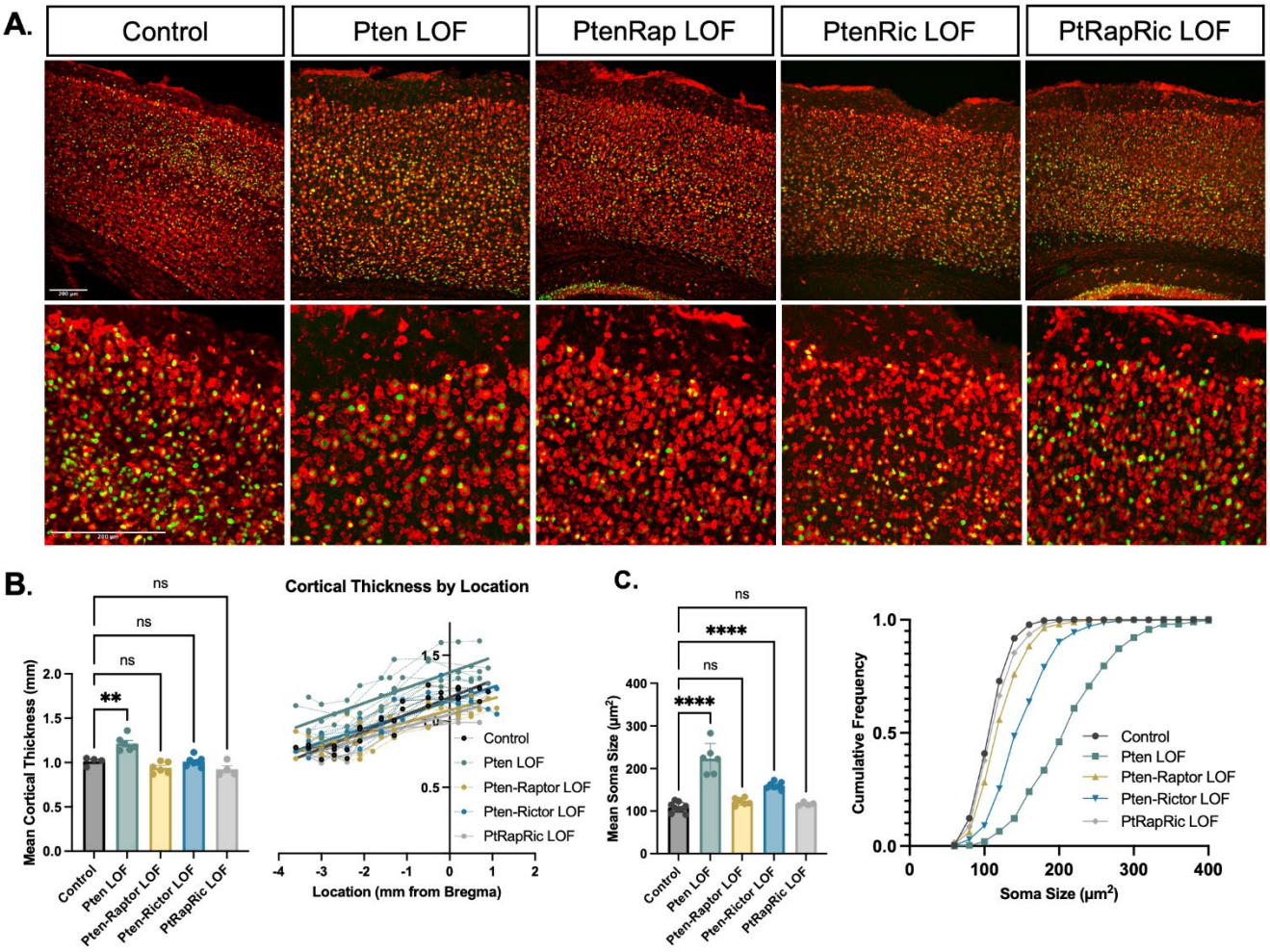

Figure 2. mTORC1 inhibition or dual mTORC1/2 inhibition rescues, and mTORC2 inhibition partially rescues, abnormalities in cortical morphology induced by focal Pten LOF.

A) Example images showing fluorescent Nissl stain (red) and GFP expression (green) in cortical neurons. The top row shows the cortical thickness in all 5 groups and the bottom row shows zoomed in images depicting the differences in soma size across groups. B) The mean cortical thickness was increased in *Pten* LOF throughout the cortex. *Pten-Raptor*, *Pten-Rictor*, and *Pten-Raptor-Rictor* LOF cortical thickness did not differ significantly from Controls. C) The mean soma size was strongly increased in *Pten* LOF and to a smaller extent in *Pten-Rictor* LOF. *Pten-Raptor* LOF and *Pten-Raptor-Rictor* LOF groups did not differ significantly from Controls. Error bars show mean ± s.e.m. ns indicates $p>0.05$, * indicates $p<0.05$, ** indicates $p<0.01$, and **** indicates $p<0.0001$ as assessed by one-way ANOVA with Tukey multiple comparisons correction.

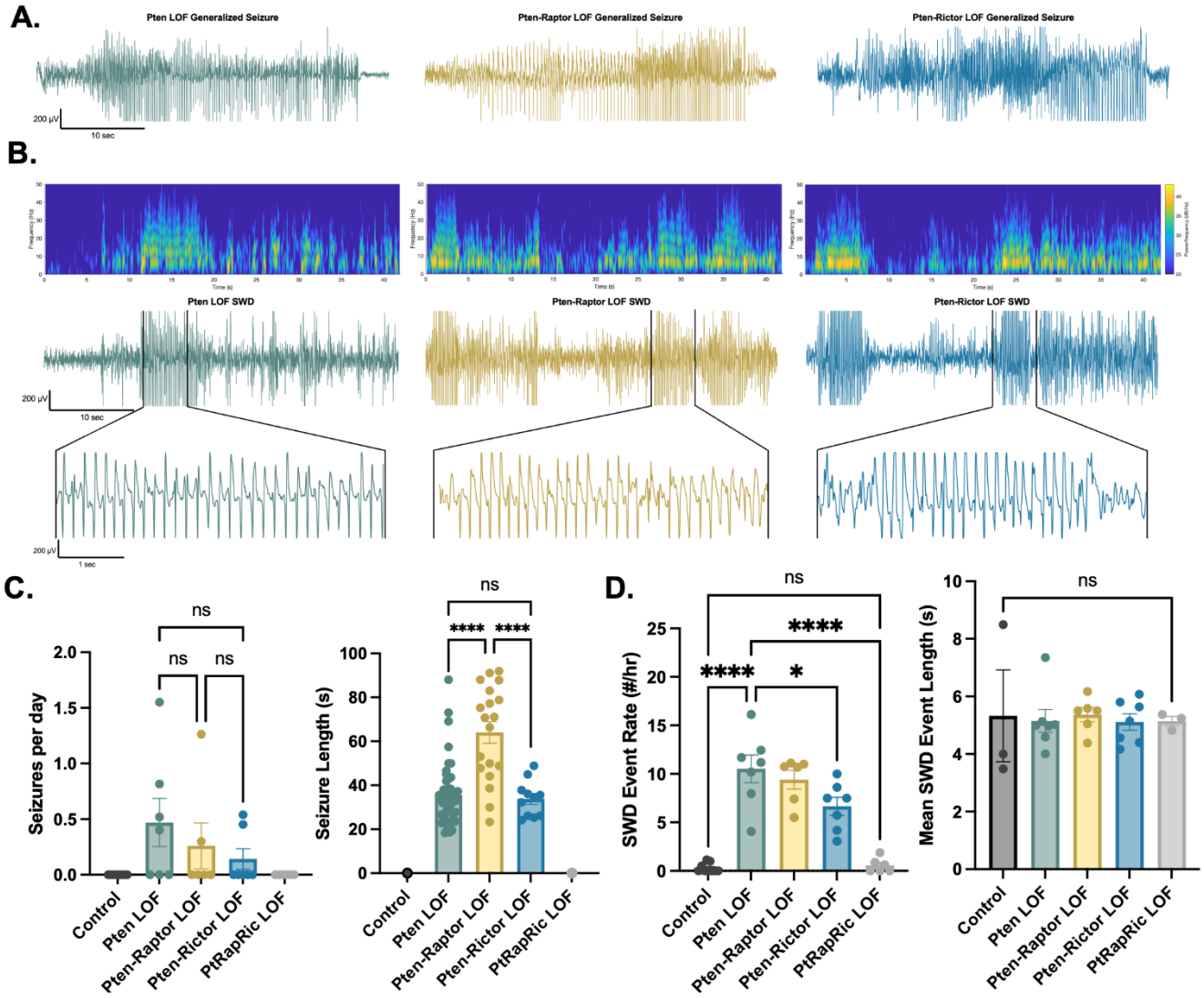

Figure 3. Combined mTORC1 and mTORC2 inactivation, but neither alone, rescues epilepsy in the focal Pten LOF model.

Spontaneous seizures and interictal spike activity were assessed in mice expressing *Pten* LOF, *Pten-Raptor* LOF, *Pten-Rictor* LOF, *Pten-Raptor-Rictor* LOF, and Controls. A) Representative traces of GS in a subset of animals in *Pten* LOF, *Pten-Raptor* LOF, and *Pten-Rictor* LOF groups. B) Spectrograms (top) and traces depicting example SWD event trains. C) Summary data showing the number of GS per day and GS length. GS events were significantly longer in the *Pten-Raptor* LOF group than the other groups. In the Pten LOF group, 19% of GS events (9/48) exceeded 45 seconds in length, and these events were observed in 2/4 Pten LOF GS+ animals. 79% of GS events (15/19) in the Pten-Raptor LOF group exceeded 45 seconds, and these events were observed in 2/2 GS+ Pten-Raptor LOF animals. 1/11 GS events in the Pten-Rictor LOF group exceeded this threshold. D. Summary data showing the SWD rate and length in all animals. Error bars show mean ± s.e.m. ns indicates $p>0.05$, * indicates $p<0.05$, ** indicates $p<0.01$, *** indicates $p<0.001$, and **** indicates $p<0.0001$ as assessed by one-way ANOVA with Tukey multiple comparisons correction.

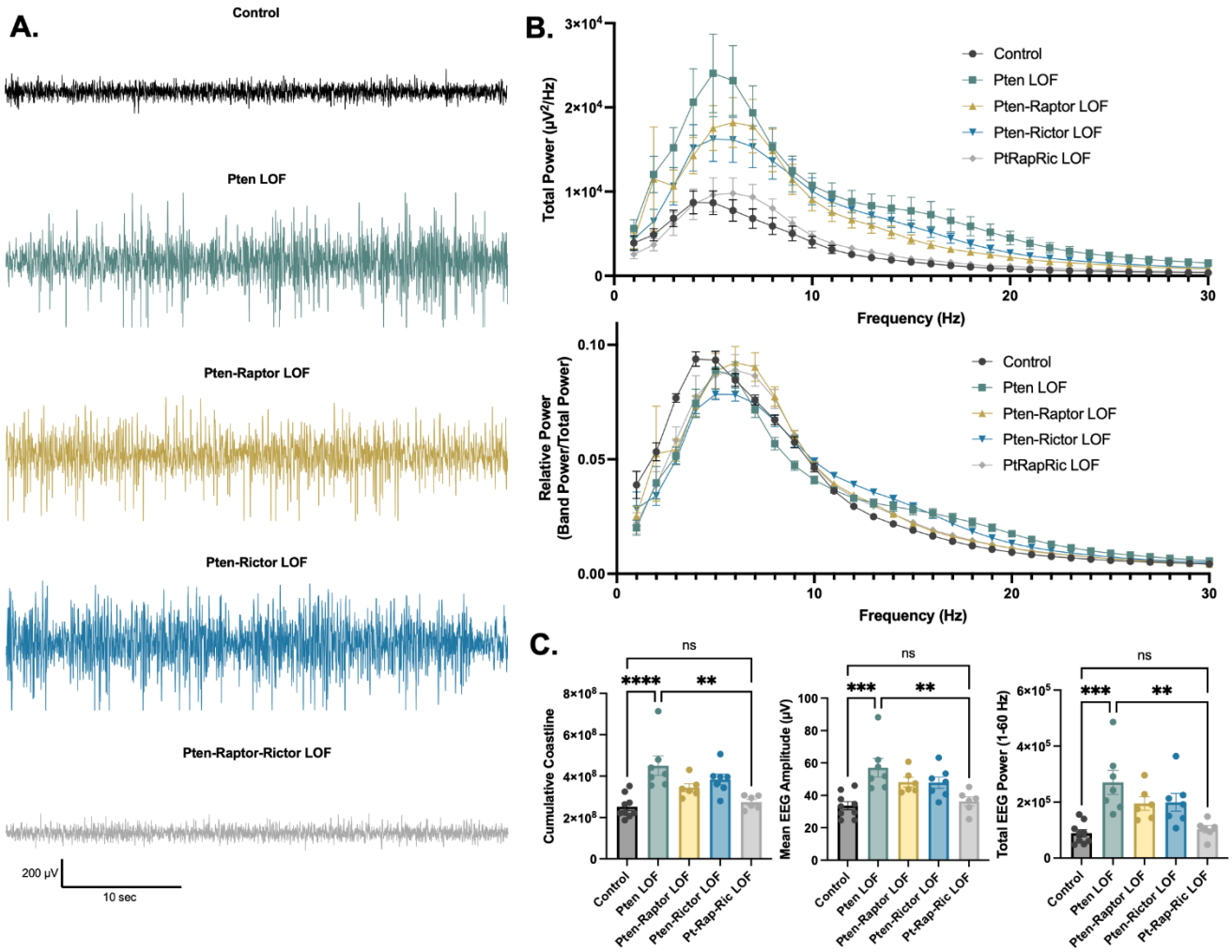

Figure 4. Combined mTORC1 and mTORC2 inactivation, but neither alone, rescues Pten LOF-induced abnormalities in the interictal EEG.

A) Examples of typical EEG traces for each genotype. In EEG epochs that were not characterized as GTCS or SWD events, *Pten* LOF animals had higher levels of EEG activity as quantified by EEG line length, absolute mean amplitude, and total power. These changes were not significantly decreased by *Raptor* LOF and *Rictor* LOF but were normalized by combined *Raptor*/*Rictor* LOF. B) Total EEG power was increased by *Pten* LOF and attenuated but not normalized by either *Raptor* or *Rictor* LOF. Relative power was decreased in delta and increased higher frequencies by *Pten* LOF. *Pten-Raptor* LOF, *Pten-Rictor* LOF, and *Pten-Raptor-Rictor* LOF animals all showed a milder rightward shift of EEG power. C) Line length, mean amplitude, and power are increased in *Pten* LOF and normalized by *Pten-Raptor-Rictor* LOF. Error bars show mean ± s.e.m. ns indicates $p>0.05$, * indicates $p<0.05$, ** indicates $p<0.01$, *** indicates $p<0.001$ as assessed by one-way ANOVA with Tukey multiple comparisons correction. Two-way ANOVA p-values for EEG power are reported in Tables 1 and 2.

Materials and Methods:

Animals: *Raptor* (Jackson Labs #013188) and *Rictor* (Jackson Labs #020649) homozygous floxed mice were crossed to a *Pten* homozygous floxed line ([43] Jackson Labs #006440). Experimental animals were the offspring of two animals homozygous floxed for *Pten* and heterozygous floxed for *Raptor* and/or *Rictor*. Intracranial viral injections were done at P0 or P1. Animals that were homozygous for the floxed *Pten* allele and either homozygous or wild-type at the *Raptor* and/or *Rictor* allele were injected with an AAV9 viral vector expressing an eGFP-Cre fusion driven by the *hSyn* promoter (Addgene #105540). Control animals were of the same genotype but were injected with an AAV9 virus expressing eGFP under control of the *hSyn* promoter, but not Cre (Addgene #105539). Pup injections were conducted with hypothermic anesthesia. A Nanoject was used to deliver 100 nL of Cre or control virus to three sites spanning the left hemisphere of the cortex. Pups were quickly rewarmed and returned to their home cage. Additional control animals with no floxed genes on a C57B6/J background (Jackson Labs #000644) were injected with the eGFP-Cre expressing AAV9 to ensure that Cre expression did not have effects independent of the $Pten^{fl/fl}$ genotype (Supplementary Figure 1).

Surgeries and EEG Recordings: Animals were aged to six weeks and then implanted with a wireless EEG monitoring headcap. Animals were anesthetized with 4% isofluorane and arranged on a stereotaxic surgical apparatus with ear bars. Anesthesia was maintained with 1.5-2.5% isofluorane. The skull surface was exposed and holes were made with a 23g needle at six locations on the skull surface. 3/32" screws (Antrin Miniature Specialties) were inserted into the holes. Screws were secured with VetBond then covered with surgical cement. The screws were attached to a six-pin Millimax strip which was secured to the skull with additional cement. Animals were administered 5 mg/kg ketoprofen post-surgery and allowed to recover for at least 5 days before EEG recording. Surgical protocol was based on guidance provided by Pinnacle Technologies (https://www.pinnaclet.com).

After recovery from surgery, animals were fitted with wireless three-channel EEG preamplifiers (Pinnacle Technologies) and EEG signal was recorded at 256 Hz with simultaneous video recording. EEG recording session length was dependent on battery life. A total of at least 150 hours of EEG data was collected for each experimental animal.

Histology and imaging: EEG-implanted animals were euthanized by isofluorane overdose followed by transcardiac perfusion with 4% paraformaldehyde. Brains were postfixed in 4% paraformaldehyde for 24 hours and then transferred to 30% sucrose for at least 48 hours. 40 µm coronal slices were cut and preserved in a cryoprotectant solution (50% PBS, 30% ethylene glycol, 20% glycerol). Prior to staining, slices were washed three times with PBS. Eight cross-sectional

unstained slices were mounted with DAPI Fluoromount-G (SouthernBiotech) and used to assess cortical thickness, GFP expression, and cell density. For other analyses, three sections per animal at approximately Bregma -1.6, -2,1, and -2.6 were used. A fluorescent Nissl stain (Invitrogen N21482, 1:50) was used to assess soma size.

After washing, slices were placed in blocking solution (10% normal goat serum, 0.1% Triton X-100, and PBS) for 1 hour. Slices were incubated in the following primary antibodies for 3 hours at room temperature: phospho-S6 Ribosomal Protein Ser240/244 (rabbit monoclonal, 1:1000 dilution, Cell Signaling Technology, catalog #5364, RRID: AB_10694233), phospho-AKT Ser473 (rabbit monoclonal, 1:1000 dilution, Cell Signaling Technology, catalog #4060), and NeuN (guinea pig polyclonal, 1:1000 dilution, Synaptic Systems, catalog #266004). Following primary antibody application, slices were washed three times in PBS and the incubated in AlexaFluor secondary antibodies goat anti-guinea pig 647 and goat anti-rabbit 594 (Invitrogen) for 1 hour at room temperature.

Slides stained for Nissl substance, NeuN/pS6, and NeuN/pAkt were imaged at 10x (2048x2048) with 5 µm z-step on a Nikon C2 confocal microscope (UVM Microscopy Imaging Core). One image of the left (GFP-expressing) cortical hemisphere in each of three region-matched slices per animal was collected for analysis. Widefield images (2560x2160) of unstained DAPI-mounted cross-sectional slices were taken with a Zyla sCMOS camera (Andor) mounted on an upright microscope (IX73; Olympus) at 5x and 20x resolution. Pixel width was manually calculated using an 0.1 mm hemocytometer.

EEG analysis: EEG files were converted from Pinnacle's proprietary format to European Data Format (EDF) files and imported to Matlab. A filtering program was used to flag traces in which seizures were likely to be occurring based on amplitude and line length between data points. For Control and Pten-Raptor-Rictor LOF animals, all 10 second epochs in which signal amplitude exceeded 400 µV at two time points at least 1 second apart were manually reviewed by a rater blinded to genotype. This method was not suitable for the Pten LOF, Pten-Raptor LOF, and Pten-Rictor LOF animals because of the density of high-amplitude interictal activity they displayed. For these animals, at least 100 of the highest-amplitude traces were manually reviewed and then traces with persistent abnormally low amplitude, often indicating postictal suppression, were reviewed as well. Flagged traces were displayed for a rater to mark the beginning and end of each seizure. Spike-and-wave discharge events were manually marked in 8 evenly spaced one-hour epochs in each of two 24-hour recording sessions per animal and verified on video not to be caused by movement such as chewing or scratching.

Baseline EEG measures were taken from a representative sample of EEG files for each animal. 692 evenly spaced five-second epochs were sampled over 24 hours, repeated for two recording

sessions per animal. Line length was defined as the sum of the linear distances between adjacent data points during the five-second analysis epoch. Mean amplitude was defined as the mean of the absolute value of data points in the five-second analysis epoch. Power spectral density was calculated with the pwelch function in Matlab. All three EEG channels were analyzed and the mean of all channels was used for statistical analysis.

Image Analysis: Image analysis was conducted using ImageJ/Fiji. Soma size was measured by dividing Nissl stain images into a 10 mm^2 grid. The somas of all GFP-expressing cells fully within three randomly selected grid squares in Layer II/III were manually traced. pS6 and pAkt expression were measured by drawing 200 µm wide columns spanning all cortical layers. Background was subtracted from images with a 30 µm rolling ball algorithm (Fiji/ImageJ). The mean pixel value of the column was recorded and values were averaged by animal.

Statistical analysis: Prism 9 (GraphPad Prism) was used to conduct statistical analyses and create graphs. Group differences were assessed using one-way ANOVA with Tukey post-hoc analysis in GraphPad9, except where noted.

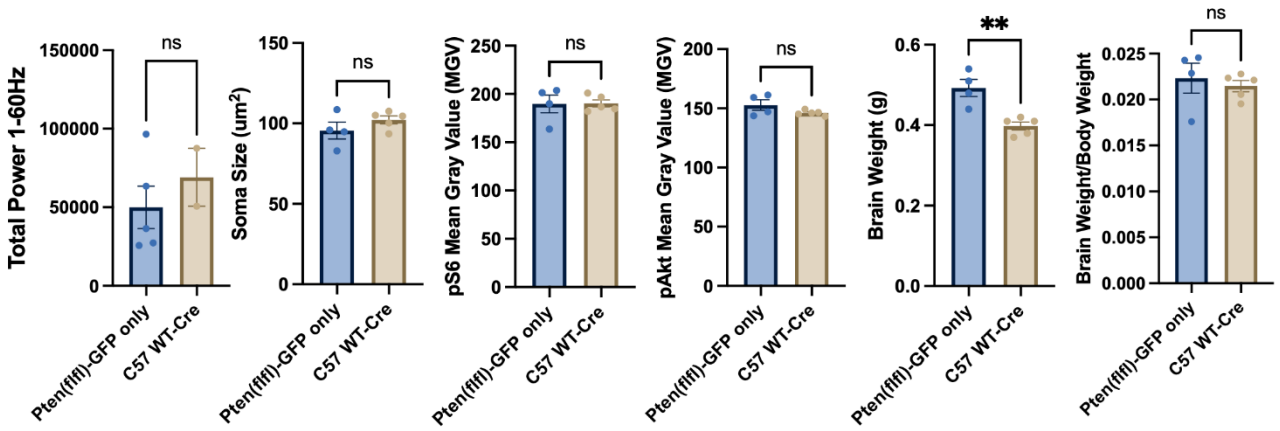

Supplementary Figure 1. Cre virus exposure does not significantly impact cortical morphology or baseline EEG. C57B6/J mice with no floxed genes were injected with the Cre virus as an additional control group. These mice did not have GS or SWDs. They were also not different from $Pten^{fl/fl}$ injected with the Control virus, except for significantly different brain weights. The brain weight/body weight ratio did not differ between the groups.

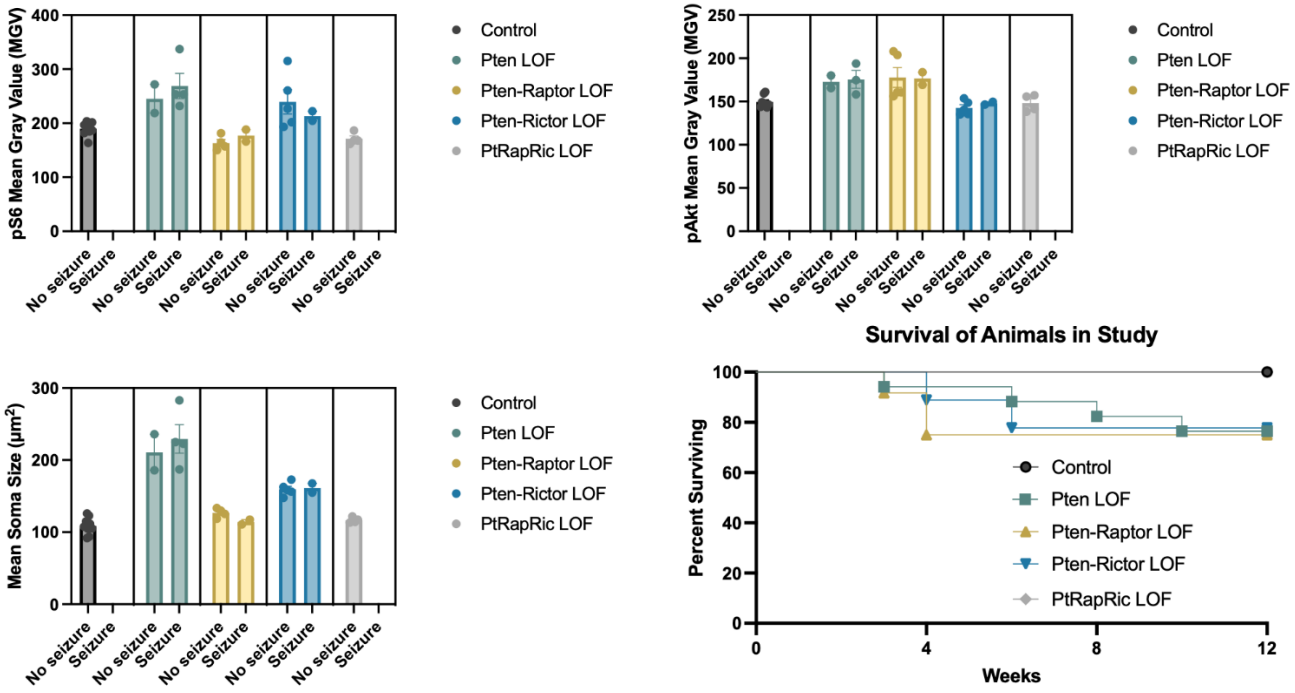

Supplementary Figure 2. Focal cortical Pten LOF, Pten-Raptor LOF, and Pten-Rictor LOF cause a spectrum of outcomes. A subset of animals in the *Pten* LOF, *Pten-Raptor* LOF, and *Pten-Rictor* LOF groups displayed spontaneous epileptiform activity, but not generalized seizures. When compared side by side, animals within each genotype that did and did not display generalized seizures showed similar mTOR pathway activity levels and soma sizes. Survival plot shows survival of animals in the study by genotype. Some animals in the *Pten* LOF, *Pten-Raptor* LOF, and *Pten-Rictor* LOF groups were found dead during the study, but no deaths were observed in Control or *Pten-Raptor-Rictor* LOF groups. Mortality often occurred prior to EEG recordings, so we could not ascertain whether early mortality was associated with generalized seizures.

References

1. Crino PB (2011) mTOR: A pathogenic signaling pathway in developmental brain malformations. Trends Mol Med 17 (12):734-742. doi:10.1016/j.molmed.2011.07.008
2. Lipton JO, Sahin M (2014) The neurology of mTOR. Neuron 84 (2):275-291. doi:10.1016/j.neuron.2014.09.034
3. Costa-Mattioli M, Monteggia LM (2013) mTOR complexes in neurodevelopmental and neuropsychiatric disorders. Nat Neurosci 16 (11):1537-1543. doi:10.1038/nn.3546
4. Wong M, Crino PB (2012) mTOR and Epileptogenesis in Developmental Brain Malformations. In: Noebels JL, Avoli M, Rogawski MA, Olsen RW, Delgado-Escueta AV (eds) Jasper's Basic Mechanisms of the Epilepsies. 4th edn., Bethesda (MD),
5. Laplante M, Sabatini DM (2012) mTOR signaling in growth control and disease. Cell 149 (2):274-293. doi:10.1016/j.cell.2012.03.017
6. Crino PB (2020) mTORopathies: A Road Well-Traveled. Epilepsy Curr 20 (6_suppl):64S-66S. doi:10.1177/1535759720959320
7. Dentel B, Escamilla CO, Tsai PT (2019) Therapeutic Targeting of mTORC2 in mTORopathies. Neuron 104 (6):1032-1033. doi:10.1016/j.neuron.2019.11.026
8. Jansen LA, Mirzaa GM, Ishak GE, O'Roak BJ, Hiatt JB, Roden WH, Gunter SA, Christian SL, Collins S, Adams C, Riviere JB, St-Onge J, Ojemann JG, Shendure J, Hevner RF, Dobyns WB (2015) PI3K/AKT pathway mutations cause a spectrum of brain malformations from megalencephaly to focal cortical dysplasia. Brain 138 (Pt 6):1613-1628. doi:10.1093/brain/awv045
9. Talos DM, Jacobs LM, Gourmaud S, Coto CA, Sun H, Lim KC, Lucas TH, Davis KA, Martinez-Lage M, Jensen FE (2018) Mechanistic target of rapamycin complex 1 and 2 in human temporal lobe epilepsy. Ann Neurol 83 (2):311-327. doi:10.1002/ana.25149

10. Weston MC, Chen H, Swann JW (2012) Multiple roles for mammalian target of rapamycin signaling in both glutamatergic and GABAergic synaptic transmission. J Neurosci 32 (33):11441-11452. doi:10.1523/JNEUROSCI.1283-12.2012
11. Williams MR, DeSpenza T, Jr., Li M, Gulledge AT, Luikart BW (2015) Hyperactivity of newborn Pten knock-out neurons results from increased excitatory synaptic drive. J Neurosci 35 (3):943-959. doi:10.1523/JNEUROSCI.3144-14.2015
12. Nguyen LH, Bordey A (2021) Convergent and Divergent Mechanisms of Epileptogenesis in mTORopathies. Front Neuroanat 15:664695. doi:10.3389/fnana.2021.664695
13. Tariq K, Cullen E, Getz SA, Conching AKS, Goyette AR, Prina ML, Wang W, Li M, Weston MC, Luikart BW (2022) Disruption of mTORC1 rescues neuronal overgrowth and synapse function dysregulated by Pten loss. Cell Rep 41 (5):111574. doi:10.1016/j.celrep.2022.111574
14. Ljungberg MC, Sunnen CN, Lugo JN, Anderson AE, D'Arcangelo G (2009) Rapamycin suppresses seizures and neuronal hypertrophy in a mouse model of cortical dysplasia. Dis Model Mech 2 (7-8):389-398. doi:10.1242/dmm.002386
15. Nguyen LH, Brewster AL, Clark ME, Regnier-Golanov A, Sunnen CN, Patil VV, D'Arcangelo G, Anderson AE (2015) mTOR inhibition suppresses established epilepsy in a mouse model of cortical dysplasia. Epilepsia 56 (4):636-646. doi:10.1111/epi.12946
16. Sunnen CN, Brewster AL, Lugo JN, Vanegas F, Turcios E, Mukhi S, Parghi D, D'Arcangelo G, Anderson AE (2011) Inhibition of the mammalian target of rapamycin blocks epilepsy progression in NS-Pten conditional knockout mice. Epilepsia 52 (11):2065-2075. doi:10.1111/j.1528-1167.2011.03280.x
17. Zhou J, Blundell J, Ogawa S, Kwon CH, Zhang W, Sinton C, Powell CM, Parada LF (2009) Pharmacological inhibition of mTORC1 suppresses anatomical, cellular, and behavioral abnormalities in neural-specific Pten knock-out mice. J Neurosci 29 (6):1773-1783. doi:10.1523/JNEUROSCI.5685-08.2009
18. Sarbassov DD, Ali SM, Sengupta S, Sheen JH, Hsu PP, Bagley AF, Markhard AL, Sabatini DM (2006) Prolonged rapamycin treatment inhibits mTORC2 assembly and Akt/PKB. Mol Cell 22 (2):159-168. doi:10.1016/j.molcel.2006.03.029
19. Angliker N, Ruegg MA (2013) In vivo evidence for mTORC2-mediated actin cytoskeleton rearrangement in neurons. Bioarchitecture 3 (4):113-118. doi:10.4161/bioa.26497
20. McCabe MP, Cullen ER, Barrows CM, Shore AN, Tooke KI, Laprade KA, Stafford JM, Weston MC (2020) Genetic inactivation of mTORC1 or mTORC2 in neurons reveals distinct functions in glutamatergic synaptic transmission. Elife 9. doi:10.7554/eLife.51440
21. Chen CJ, Sgritta M, Mays J, Zhou H, Lucero R, Park J, Wang IC, Park JH, Kaipparettu BA, Stoica L, Jafar-Nejad P, Rigo F, Chin J, Noebels JL, Costa-Mattioli M (2019) Therapeutic inhibition of mTORC2 rescues the behavioral and neurophysiological abnormalities associated with Pten-deficiency. Nat Med 25 (11):1684-1690. doi:10.1038/s41591-019-0608-y
22. Cullen ER, Tariq K, Shore AN, Luikart BW, Weston MC (2023) mTORC2 Inhibition Improves Morphological Effects of PTEN Loss, But Does Not Correct Synaptic Dysfunction or Prevent Seizures. J Neurosci 43 (5):827-845. doi:10.1523/JNEUROSCI.1354-22.2022
23. Kim JK, Lee JH (2019) Mechanistic Target of Rapamycin Pathway in Epileptic Disorders. J Korean Neurosurg Soc 62 (3):272-287. doi:10.3340/jkns.2019.0027
24. Koboldt DC, Miller KE, Miller AR, Bush JM, McGrath S, Leraas K, Crist E, Fair S, Schwind W, Wijeratne S, Fitch J, Leonard J, Shaikhouni A, Hester ME, Magrini V, Ho ML, Pierson CR, Wilson RK, Ostendorf AP, Mardis ER, Bedrosian TA (2021) PTEN somatic mutations contribute to spectrum of cerebral overgrowth. Brain 144 (10):2971-2978. doi:10.1093/brain/awab173
25. Chen Y, Huang WC, Sejourne J, Clipperton-Allen AE, Page DT (2015) Pten Mutations Alter Brain Growth Trajectory and Allocation of Cell Types through Elevated beta-Catenin Signaling. J Neurosci 35 (28):10252-10267. doi:10.1523/JNEUROSCI.5272-14.2015
26. Lasarge CL, Danzer SC (2014) Mechanisms regulating neuronal excitability and seizure development following mTOR pathway hyperactivation. Front Mol Neurosci 7:18. doi:10.3389/fnmol.2014.00018
27. Zahedi Abghari F, Moradi Y, Akouchekian M (2019) PTEN gene mutations in patients with macrocephaly and classic autism: A systematic review. Med J Islam Repub Iran 33:10. doi:10.34171/mjiri.33.10

28. Kwon CH, Zhu X, Zhang J, Baker SJ (2003) mTor is required for hypertrophy of Pten-deficient neuronal soma in vivo. Proc Natl Acad Sci U S A 100 (22):12923-12928. doi:10.1073/pnas.2132711100
29. Cortez MA, Wu Y, Gibson KM, Snead OC, 3rd (2004) Absence seizures in succinic semialdehyde dehydrogenase deficient mice: a model of juvenile absence epilepsy. Pharmacol Biochem Behav 79 (3):547-553. doi:10.1016/j.pbb.2004.09.008
30. Moloney PB, Cavalleri GL, Delanty N (2021) Epilepsy in the mTORopathies: opportunities for precision medicine. Brain Commun 3 (4):fcab222. doi:10.1093/braincomms/fcab222
31. Griffith JL, Wong M (2018) The mTOR pathway in treatment of epilepsy: a clinical update. Future Neurol 13 (2):49-58. doi:10.2217/fnl-2018-0001
32. French JA, Lawson JA, Yapici Z, Ikeda H, Polster T, Nabbout R, Curatolo P, de Vries PJ, Dlugos DJ, Berkowitz N, Voi M, Peyrard S, Pelov D, Franz DN (2016) Adjunctive everolimus therapy for treatment-resistant focal-onset seizures associated with tuberous sclerosis (EXIST-3): a phase 3, randomised, double-blind, placebo-controlled study. Lancet 388 (10056):2153-2163. doi:10.1016/S0140-6736(16)31419-2
33. Karalis V, Caval-Holme F, Bateup HS (2022) Raptor downregulation rescues neuronal phenotypes in mouse models of Tuberous Sclerosis Complex. Nat Commun 13 (1):4665. doi:10.1038/s41467-022-31961-6
34. Nguyen LH, Xu Y, Mahadeo T, Zhang L, Lin TV, Born HA, Anderson AE, Bordey A (2022) Expression of 4E-BP1 in juvenile mice alleviates mTOR-induced neuronal dysfunction and epilepsy. Brain 145 (4):1310-1325. doi:10.1093/brain/awab390
35. Lyu J, Yu X, He L, Cheng T, Zhou J, Cheng C, Chen Z, Cheng G, Qiu Z, Zhou W (2015) The protein phosphatase activity of PTEN is essential for regulating neural stem cell differentiation. Mol Brain 8:26. doi:10.1186/s13041-015-0114-1
36. Angliker N, Burri M, Zaichuk M, Fritschy JM, Ruegg MA (2015) mTORC1 and mTORC2 have largely distinct functions in Purkinje cells. Eur J Neurosci 42 (8):2595-2612. doi:10.1111/ejn.13051
37. Choo AY, Blenis J (2009) Not all substrates are treated equally: implications for mTOR, rapamycin-resistance and cancer therapy. Cell Cycle 8 (4):567-572. doi:10.4161/cc.8.4.7659
38. Kim DH, Sarbassov DD, Ali SM, King JE, Latek RR, Erdjument-Bromage H, Tempst P, Sabatini DM (2002) mTOR interacts with raptor to form a nutrient-sensitive complex that signals to the cell growth machinery. Cell 110 (2):163-175. doi:10.1016/s0092-8674(02)00808-5
39. Schreiber KH, Arriola Apelo SI, Yu D, Brinkman JA, Velarde MC, Syed FA, Liao CY, Baar EL, Carbajal KA, Sherman DS, Ortiz D, Brunauer R, Yang SE, Tzannis ST, Kennedy BK, Lamming DW (2019) A novel rapamycin analog is highly selective for mTORC1 in vivo. Nat Commun 10 (1):3194. doi:10.1038/s41467-019-11174-0
40. Theilmann W, Gericke B, Schidlitzki A, Muneeb Anjum SM, Borsdorf S, Harries T, Roberds SL, Aguiar DJ, Brunner D, Leiser SC, Song D, Fabbro D, Hillmann P, Wymann MP, Loscher W (2020) Novel brain permeant mTORC1/2 inhibitors are as efficacious as rapamycin or everolimus in mouse models of acquired partial epilepsy and tuberous sclerosis complex. Neuropharmacology 180:108297. doi:10.1016/j.neuropharm.2020.108297
41. Roy A, Skibo J, Kalume F, Ni J, Rankin S, Lu Y, Dobyns WB, Mills GB, Zhao JJ, Baker SJ, Millen KJ (2015) Mouse models of human PIK3CA-related brain overgrowth have acutely treatable epilepsy. Elife 4. doi:10.7554/eLife.12703
42. White AR, Tiwari D, MacLeod MC, Danzer SC, Gross C (2020) PI3K isoform-selective inhibition in neuron-specific PTEN-deficient mice rescues molecular defects and reduces epilepsy-associated phenotypes. Neurobiol Dis 144:105026. doi:10.1016/j.nbd.2020.105026
43. Groszer M, Erickson R, Scripture-Adams DD, Lesche R, Trumpp A, Zack JA, Kornblum HI, Liu X, Wu H (2001) Negative regulation of neural stem/progenitor cell proliferation by the Pten tumor suppressor gene in vivo. Science 294 (5549):2186-2189. doi:10.1126/science.1065518

Acknowledgements: Research reported in this publication was supported by NINDS grant R01NS110945 (M.C.W.), as well as P20GM135007, Core C: Customized Physiology and Imaging Core. Images created with BioRender. We thank Caitlynn Barrows, Elise Prehoda, and Willie Tobin for early experiments helping create the mouse model.

Table 1. EEG power

Table 1A: Total Power

Band	2-way ANOVA p-value						
	Control vs. Pten LOF	Control vs. Pten-Raptor LOF	Control vs. Pten-Rictor LOF	Control vs. Pten-Raptor-Rictor LOF	Pten LOF vs. Pten-Raptor LOF	Pten LOF vs. Pten-Rictor LOF	Pten LOF vs. Pten-Raptor-Rictor LOF
1	0.7215	0.9996	0.9976	0.7021	0.8249	0.9347	0.1485
2	0.0833	0.8162	0.8509	0.7749	>0.9999	0.276	0.043
3	0.0657	0.4328	0.5564	0.9949	0.5893	0.6387	0.0543
4	0.1205	0.2658	0.3091	>0.9999	0.6358	0.79	0.1219
5	0.0834	0.1019	0.1838	0.9946	0.7452	0.6116	0.1144
6	0.0508	0.0779	0.127	0.8868	0.8606	0.6302	0.0988
7	0.0395	0.0829	0.0875	0.6727	0.9963	0.8508	0.1137
8	0.0321	0.0749	0.0746	0.6353	>0.9999	0.9834	0.1093
9	0.0236	0.0727	0.0766	0.8311	0.9923	0.9993	0.0576
10	0.0156	0.0605	0.0609	0.9112	0.9096	0.9974	0.0297
11	0.0148	0.0469	0.0336	0.8046	0.7577	0.9889	0.0275
12	0.017	0.0376	0.0186	0.5816	0.7035	0.9837	0.0321
13	0.0219	0.0431	0.0138	0.5078	0.6552	0.9572	0.0379
14	0.0322	0.0298	0.0109	0.5927	0.4738	0.9128	0.0486
15	0.047	0.0172	0.0087	0.7629	0.35	0.8344	0.0616
16	0.0497	0.0133	0.0081	0.5221	0.2767	0.7401	0.0669
17	0.0386	0.0092	0.0104	0.4807	0.2108	0.6195	0.0524
18	0.0284	0.0104	0.0129	0.4624	0.1732	0.4864	0.0386
19	0.0241	0.0166	0.0139	0.607	0.1619	0.3975	0.0315
20	0.0221	0.0132	0.0179	0.3517	0.1556	0.368	0.0342
21	0.021	0.008	0.0176	0.3236	0.1487	0.3703	0.0334
22	0.0238	0.0078	0.0188	0.3161	0.1752	0.4039	0.0382
23	0.0279	0.0093	0.021	0.3728	0.2164	0.4387	0.0434
24	0.0303	0.0131	0.0247	0.4069	0.2433	0.4609	0.0463
25	0.0314	0.0191	0.0253	0.3983	0.2521	0.4648	0.0479
26	0.0366	0.0144	0.026	0.4339	0.2631	0.4714	0.0552
27	0.0399	0.0079	0.0264	0.4669	0.2576	0.4914	0.0599
28	0.0463	0.0064	0.0273	0.4853	0.2697	0.5059	0.0687
29	0.0559	0.0122	0.0282	0.4671	0.3075	0.5461	0.0831
30	0.0598	0.0141	0.0287	0.4514	0.3209	0.5616	0.0894

Table 1B: Relative Power

Band	2-way ANOVA p-value						
	Control vs. Pten LOF	Control vs. Pten-Raptor LOF	Control vs. Pten-Rictor LOF	Control vs. Pten-Raptor-Rictor LOF	Pten LOF vs. Pten-Raptor LOF	Pten LOF vs. Pten-Rictor LOF	Pten LOF vs. Pten-Raptor-Rictor LOF
1	<0.0001	<0.0001	0.0033	<0.0001	0.4967	0.0572	0.9743
2	<0.0001	0.9986	<0.0001	<0.0001	0.0009	0.3614	0.9977
3	<0.0001	<0.0001	<0.0001	<0.0001	0.9337	0.9777	0.2279
4	<0.0001	<0.0001	<0.0001	<0.0001	0.997	0.8997	0.9044

5	0.5938	0.4988	<0.0001	0.1852	>0.9999	0.0063	0.9593
6	0.9826	0.0834	0.189	0.5724	0.3384	0.0796	0.9046
7	0.6153	<0.0001	0.9878	0.0043	<0.0001	0.8905	<0.0001
8	0.0053	0.0074	>0.9999	0.0208	<0.0001	0.0114	<0.0001
9	0.0065	0.9007	0.9998	0.832	0.0006	0.0053	0.0003
10	0.3806	0.9964	0.8873	0.9994	0.2612	0.0714	0.3248
11	>0.9999	0.8412	0.1377	0.9282	0.9154	0.2466	0.9685
12	0.7573	0.4594	0.0076	0.6587	0.9923	0.2905	0.9999
13	0.2732	0.3278	0.002	0.5321	>0.9999	0.5486	0.994
14	0.086	0.6136	0.0015	0.6451	0.8414	0.8216	0.819
15	0.0278	0.8819	0.0033	0.7984	0.3346	0.9894	0.4322
16	0.0089	0.9533	0.0105	0.9064	0.1119	0.9998	0.1569
17	0.0059	0.9659	0.0539	0.9184	0.0744	0.9312	0.1137
18	0.0062	0.9594	0.1831	0.9362	0.0828	0.7147	0.1027
19	0.0162	0.9653	0.4248	0.9619	0.1467	0.6116	0.152
20	0.0594	0.9772	0.6562	0.9777	0.2931	0.6739	0.2915
21	0.1876	0.9896	0.8068	0.9836	0.5003	0.8099	0.5378
22	0.397	0.9948	0.9024	0.9905	0.706	0.9022	0.7437
23	0.5863	0.996	0.9476	0.9958	0.8445	0.9485	0.8465
24	0.7443	0.998	0.972	0.998	0.9163	0.975	0.9174
25	0.8341	0.9992	0.9844	0.9988	0.9447	0.9851	0.9517
26	0.8939	0.9997	0.9931	0.9992	0.9617	0.9887	0.972
27	0.9375	>0.9999	0.9965	0.9995	0.9721	0.9934	0.9851
28	0.9652	>0.9999	0.9981	0.9996	0.9815	0.9967	0.993
29	0.9801	>0.9999	0.9988	0.9996	0.9879	0.9983	0.9972
30	0.9886	>0.9999	0.9993	0.9995	0.9922	0.9991	0.9991